Electronic Supplementary Material (ESI) for Sustainable Energy & Fuels.
This journal is © The Royal Society of Chemistry 2023

Supplementary Information

Enabling a Rapid SnO_2 Chemical Bath Deposition Process for Perovskite Solar Cells

Darrell Jun Jie Tay[a,b], Benny Febriansyah[a], Teddy Salim[c], Zi Sheng Wong[c], Herlina Arianita Dewi[a], Teck Ming Koh[a], and Nripan Mathews[a,c]

[a.] Energy Research Institute @ NTU (ERI@N), Nanyang Technological University, Singapore 637553, Singapore.

[b.] Interdisciplinary Graduate Programme (IGP), Graduate College, Nanyang Technological University, Singapore 637460, Singapore.

[c.] School of Materials Science and Engineering, Nanyang Technological University, Singapore 639798, Singapore

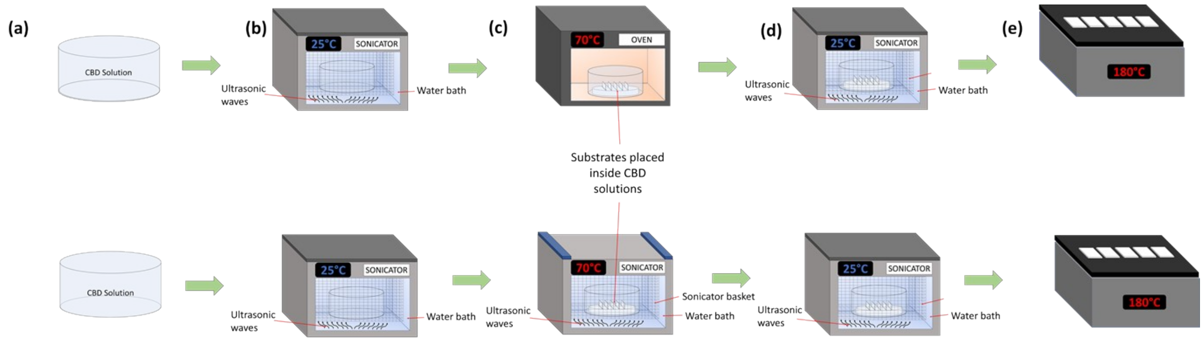

Figure S1. Schematic diagram of the process. **(a)** CBD solution is prepared. **(b)** Solution is first sonicated as a mixing step **(c)** Substrates are then placed in the bath, and the entire bath is either placed in an oven, or a sonicator **(d)** Substrates are rinsed in DI water and sonicated to remove large agglomerations **(e)** Substrates are then annealed on a hotplate.

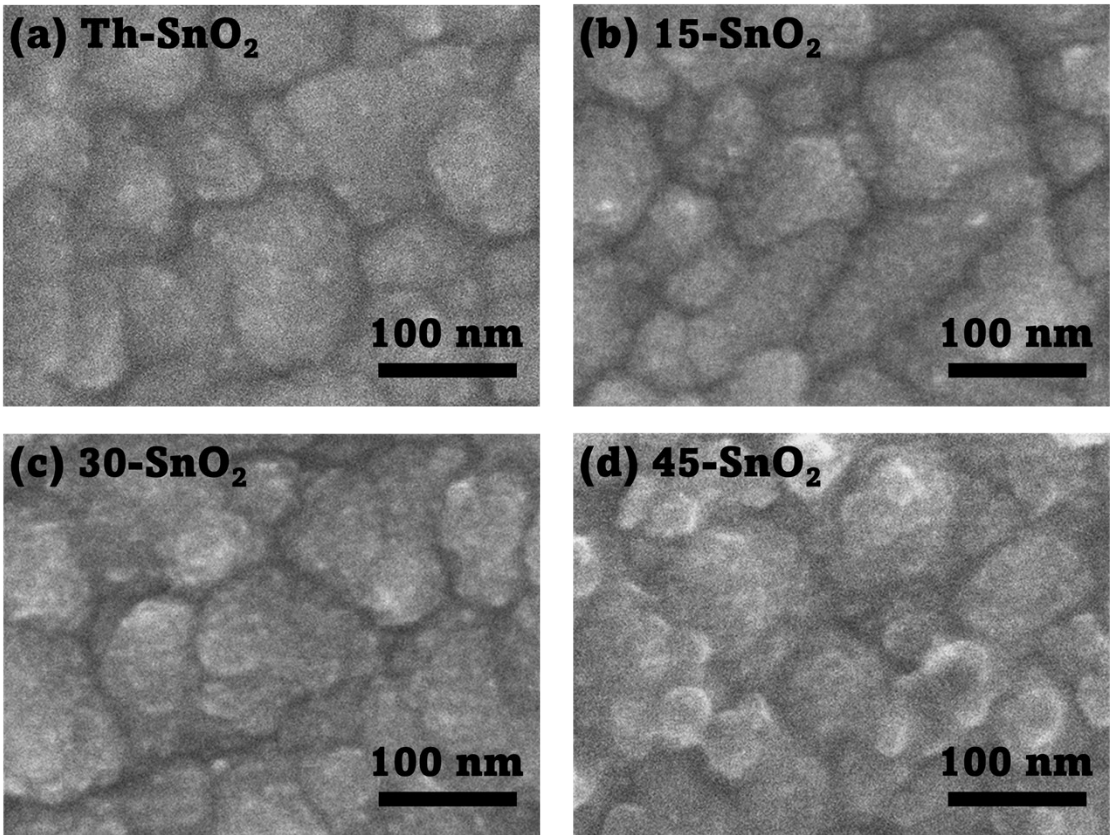

Figure S2. Top-view SEM images of films of **(a)** Th-SnO$_2$ **(b)** 15-SnO$_2$ **(c)** 30-SnO$_2$ **(d)** 45-SnO$_2$

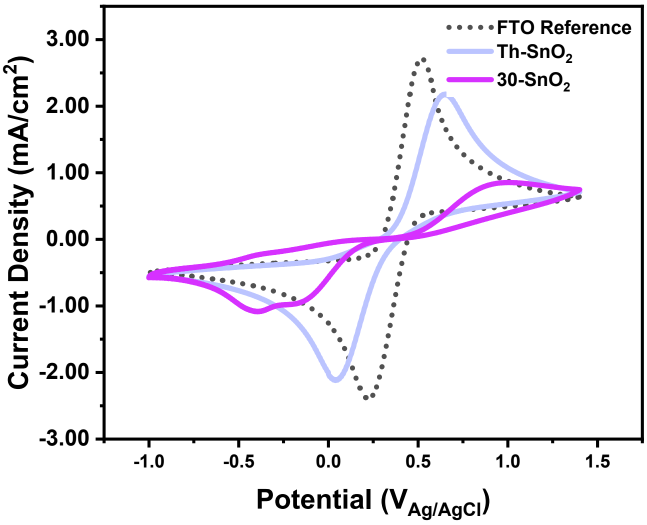

Figure S3. Corresponding cyclic-voltammetry graph for Figure 2c, indicating better coverage with 30 minutes of sonication as opposed to the 30 minutes of standard CBD in the oven.

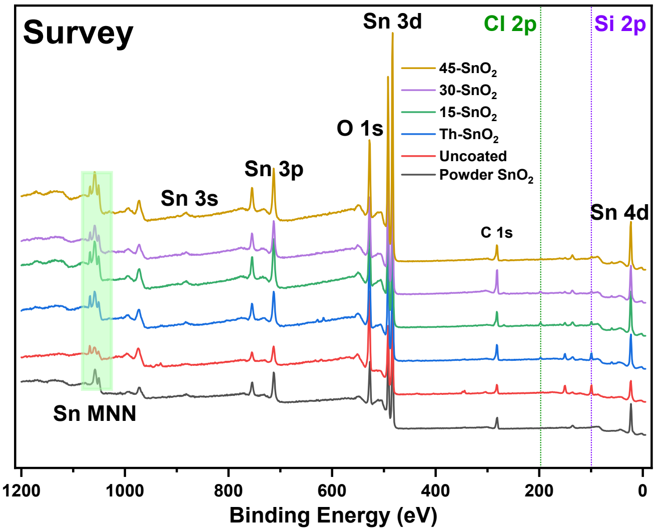

Figure S4. Complete XPS Survey scan.

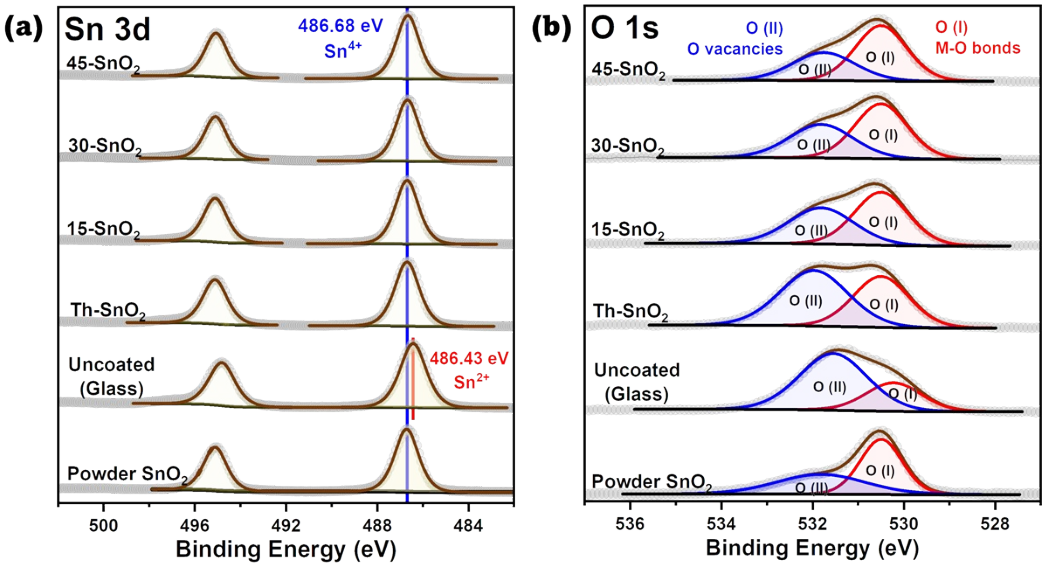

Figure S5. Complete XPS data with Th-SnO_2 and powdered SnO_2 for **(a)** Sn 3d **(b)** O 1s. All Sn 3d peaks had signatures of Sn^{4+}, except for the uncoated glass substrate.

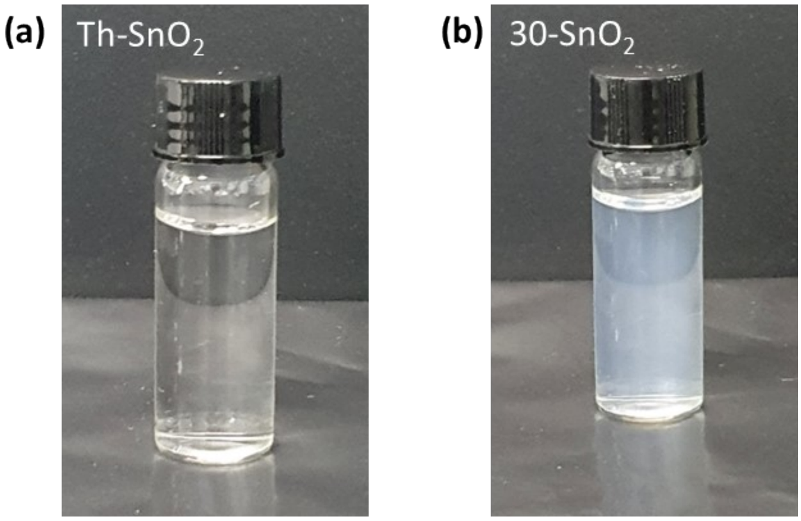

Figure S6. Appearance of the CBD solutions after the CBD process was halted.

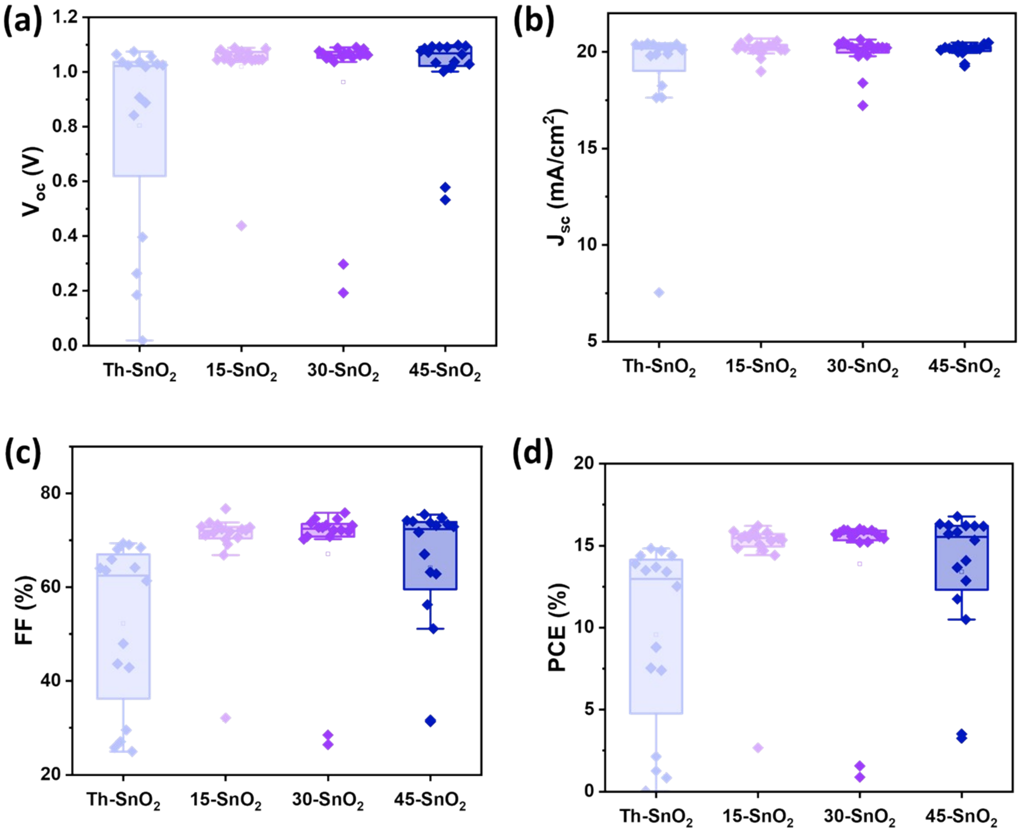

Figure S7. Boxplots of all devices. **(a)** V_{oc} **(b)** J_{sc} **(c)** FF **(d)** PCE. Most of the data points for **(d)** falls in two general regions (15-SnO_2, 30-SnO_2, 45-SnO_2) or three regions (Th-SnO_2) for each ETL However, for all ETL types, most of the data points lie above 10% PCE. Hence, 10% was used as the benchmark for a working cell, and cells with < 10% PCE were considered failed cells, and these cells were removed from **Figures 4a-e** in the main report. Total number of cells removed: Th-SnO_2: 7/16, 15-SnO_2: 1/16, 30-SnO_2: 2/16, 45-SnO_2: 2/16.

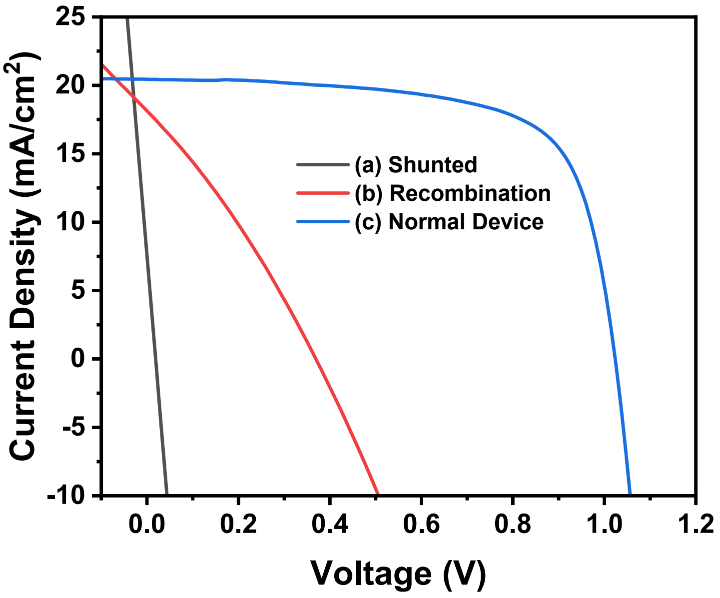

Figure S8. Examples of JV-curves of **(a)** Shunted devices **(b)** Devices likely with high degree of recombination losses with low V_{oc} and low FF. Note that the Jsc is close to that of the normal working device **(c)** Normal working device. All three devices were fabricated from Th-SnO_2 films.

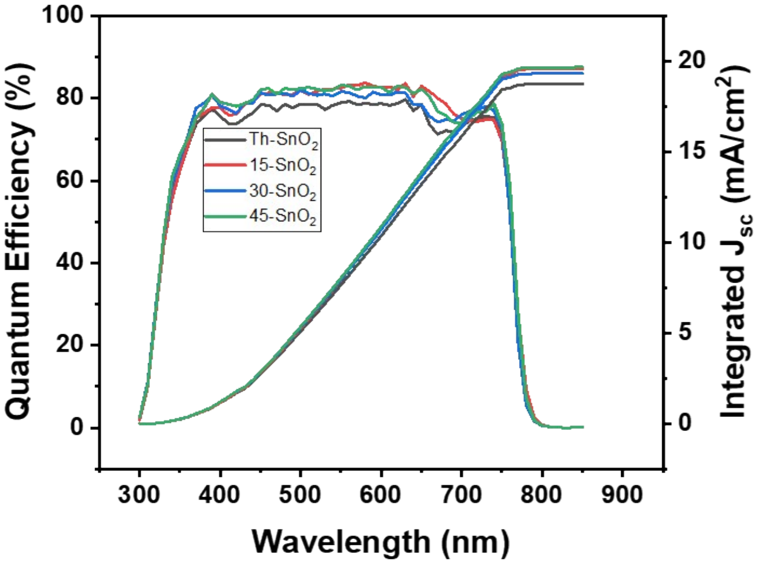

Figure S9. IPCE spectra and integrated J_{sc}.

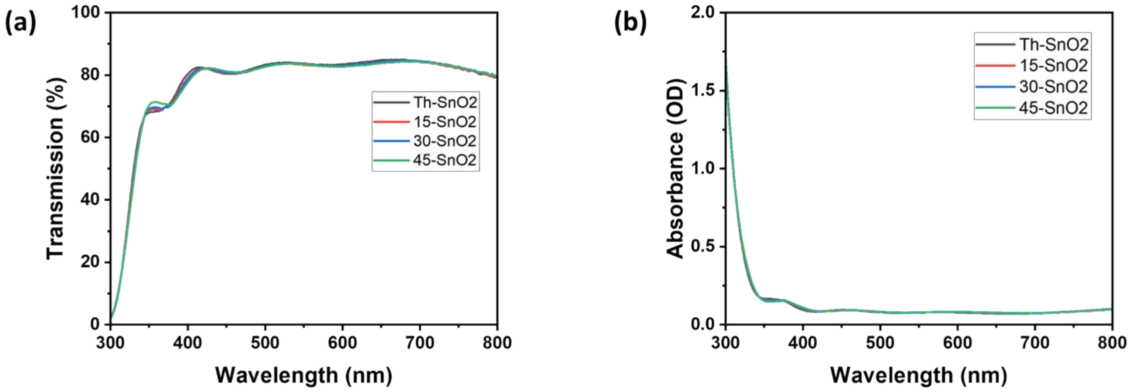

Figure S10. (a) Transmission spectra **(b)** Absorbance spectra

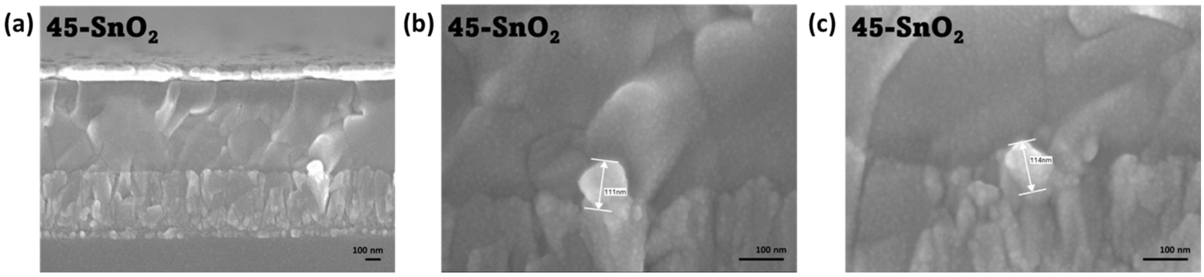

Figure S11: (a) Cross-sectional SEM image of 45-SnO_2, showing a single white precipitate on the interface of the FTO and perovskite. **(b)** A close-up view of (a). **(c)** Another particle found in the interface.

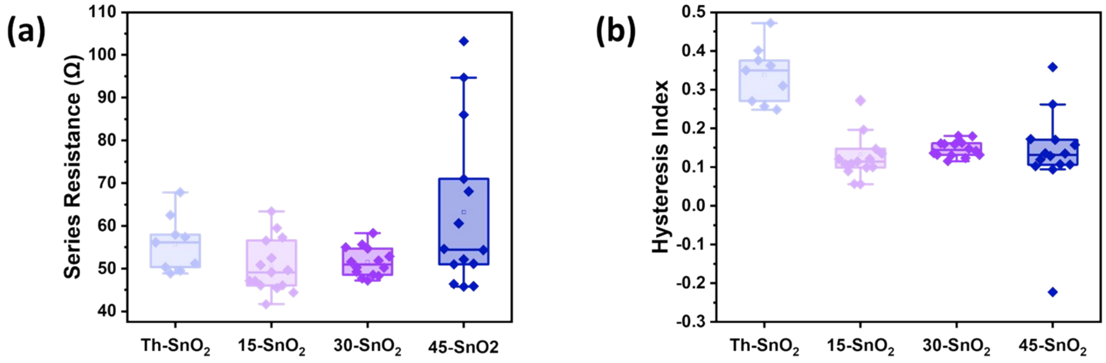

Figure S12. Boxplots of **(a)** Estimated series resistance **(b)** Hysteresis index of devices with PCE higher than 10%.

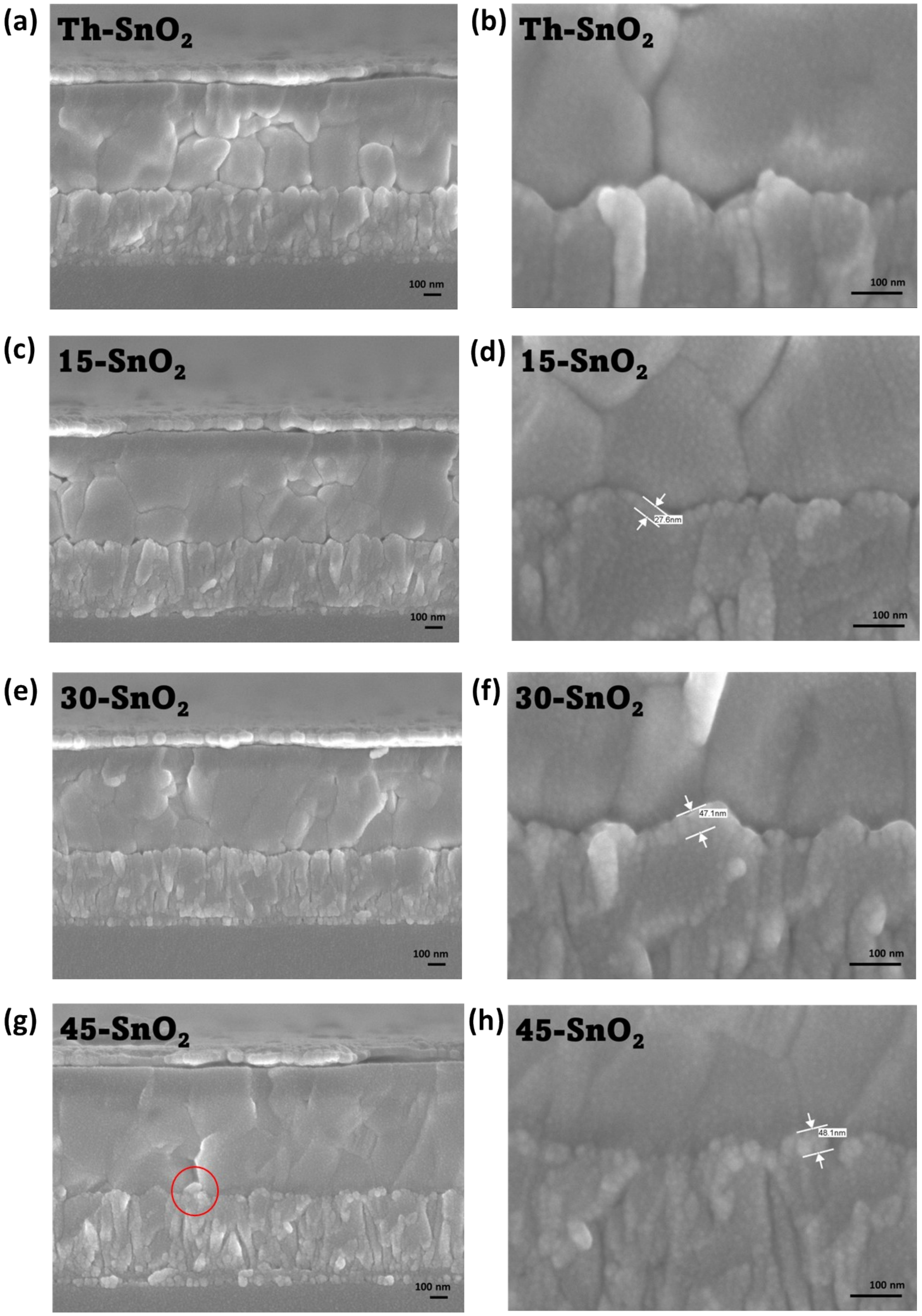

Figure S13: **(a)** – **(h)** Cross-sectional SEM images of devices. Note that **(g)** also shows one agglomerated particle between the FTO and the perovskite layer, circled in red.

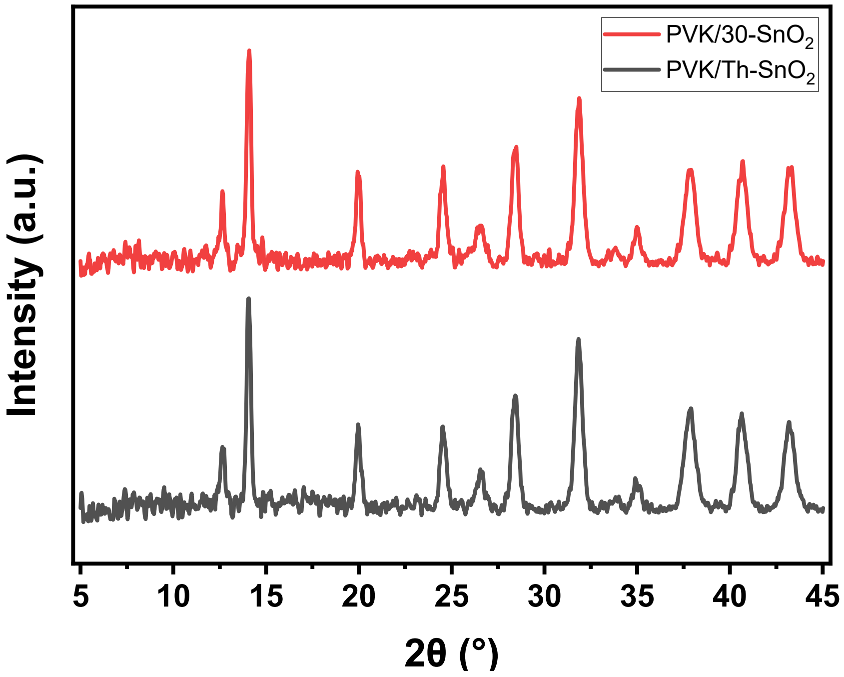

Figure S14: 1D XRD Spectra of perovskite coated on 30-SnO$_2$ and Th-SnO$_2$.

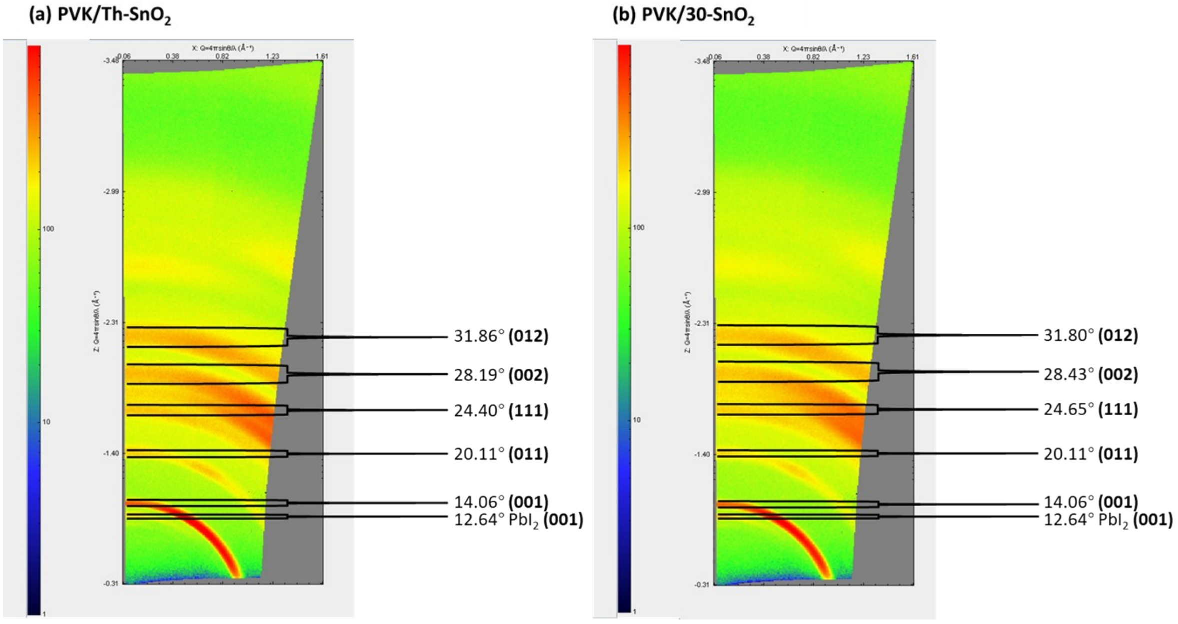

Figure S15. 2D GIWAXS of perovskite coated on 30-SnO$_2$ and Th-SnO$_2$, showing similar grain orientations. Miller indices of triple cation perovskite are from Alanazi et al. [1], and Miller index for PbI$_2$ (001) was referenced from Silva Filho et al. [2]

Comparative Study with Colloidal-SnO_2 ETL

Commercially-available colloidal-SnO_2 is one of many alternatives for depositing a layer of SnO_2 ETL, with the earliest use by Jiang and co-workers[3] back in 2018. Here, to benchmark our ultrasonication-assisted CBD approach, devices made from colloidal-SnO_2 were fabricated, following the methodology employed by Jiang and co-workers. **Figure S18** below shows the various solar cell parameters for devices based on the two ETL deposition techniques.

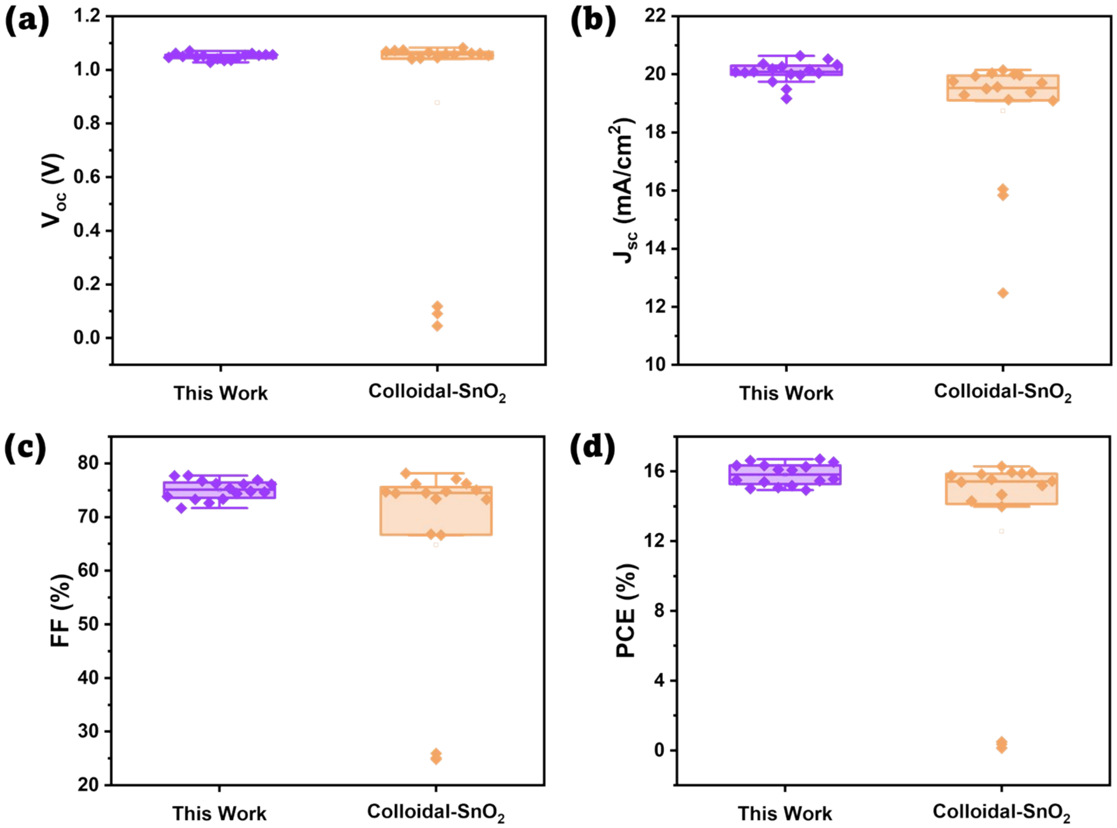

Figure S16. Comparison of devices made from ultrasonication-assisted CBD ("This Work") and commercially-available colloidal SnO_2, following the methodology by Jiang and co-workers[3].

In **Figure S16**, all devices are represented in the boxplots, and while the PCE for colloidal-SnO_2-based devices were slightly lower than that of the ultrasonicated ones (owing to higher J_{sc} and FF values), the device performances are largely comparable. However, it is apparent that there are 2 shunted devices based on the colloidal-SnO_2 ETL. As discussed in the main report and by Anaraki and co-workers[4], shunts are indicative of poor coverage of SnO_2, which would affect reproducibility of device fabrication. Therefore, we believe that this highlights the strength of our ultrasonication-assisted CBD approach, over the spincoating method of colloidal-SnO_2. However, we do not rule out the possibility that the coverage for colloidal-SnO_2 films can be improved via optimisations, or through a different deposition technique, such as slot-die coating[5].

Comparative Study with different $SnCl_2$ concentrations

In this work, the concentration of the CBD precursor solution was 0.0033M, which is different from the concentrations used by Anaraki and co-workers (0.012M and 0.002M). This value is based on optimsations done in our laboratory. Another comparative study was designed to observe the effects of increasing the concentration of $SnCl_2$ on the device performance. We note that Ko and co-workers have claimed that better SnO_2 coverage is possible when using higher concentrations of $SnCl_2$ in the CBD precursor (0.120M)[6]. Therefore, three concentrations were tested – 0.0033M, 0.012M and 0.12M. **Figure S16** below shows the CBD solutions before and after 30 minutes of CBD with ultrasonication.

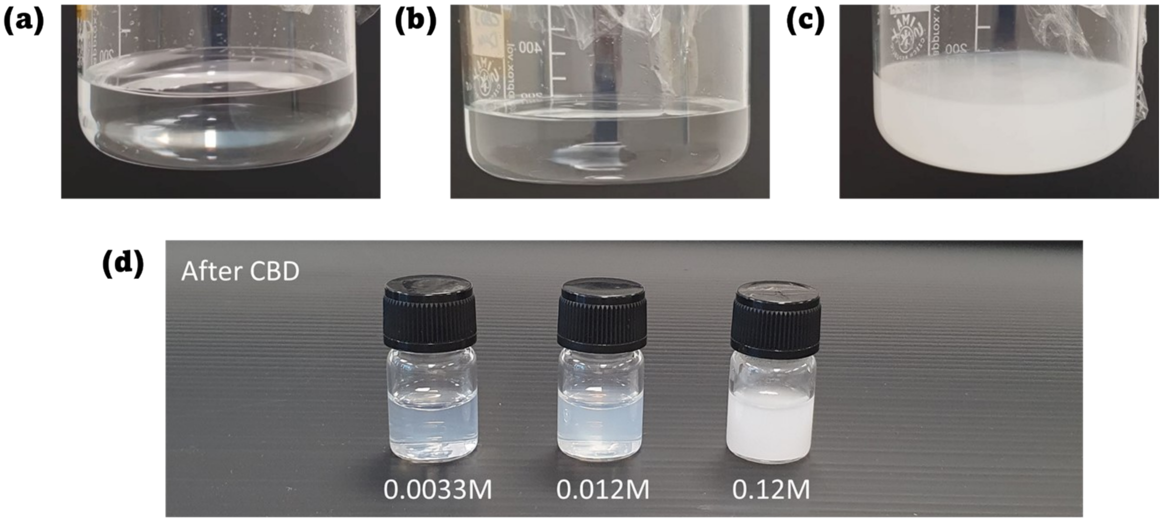

Figure S17. (a-c) CBD solutions before CBD deposition, and before substrates were placed inside. **(a)** 0.0033M **(b)** 0.012M **(c)** 0.12M. **(d)** Solutions after the CBD process.

Unlike the other two solutions, the 0.12M solution did not dissolve fully. This is likely due to the excess $SnCl_2$. Adding the HCl helps the $SnCl_2$ dissociate into free Sn^{2+} ions[7], so the appearance of precipitates suggests that $SnCl_2$ is hydrolysing, indicating a lack of HCl relative to the amount of $SnCl_2$ present. To avoid tuning multiple parameters at once, the amount of HCl added to the three solutions were kept the same, and the cloudy solution was used for fabricating the devices. We note that Ko et al. dissolved $SnCl_2$ in ethanol before dilution[6], and perhaps this may have allowed the eventual tin precursor to remain dissolved in the solution. Unsurprisingly, after 30 minutes of CBD (for all three concentrations), the solutions had different turbidity, where turbidity increased with initial concentration of $SnCl_2$.

Figure S18 below shows device data for devices fabricated from the three different concentrations.

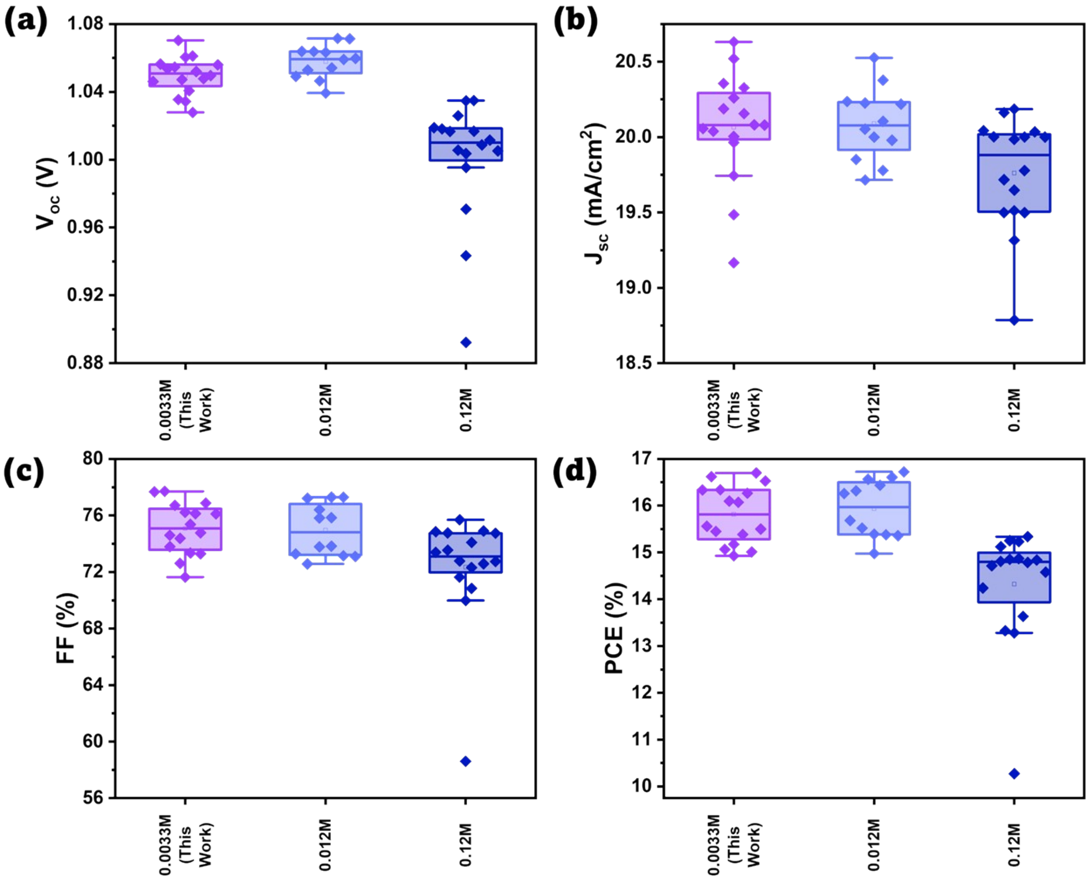

Figure S18. Device data for films formed with the three different concentrations. **(a)** Voc **(b)** Jsc **(c)** FF **(d)** PCE.

All devices were functional (i.e. no shunts or severe recombinations). Devices based on the 0.12M CBD solution had suppressed V_{oc}, J_{sc}, and FF, and consequently PCE was suppressed as compared to the devices based on the other two concentrations. This is expected, since 45-SnO_2 also showed similar results – excessive CBD produces poor film morphologies (Figure S2) that likely contributed to greater interfacial defects and poorer contact. This is likely the case for 0.12M, since increasing the concentration of $SnCl_2$ also increases the speed of the CBD reaction, and thus 30 minutes may have been too long for the 0.12M solution.

Between 0.0033M ("This work") and 0.012M, while V_{oc} values are higher for 0.012M, leading to a slightly higher median PCE of 15.97% (compared to 15.82% for 0.0033M), the increase in PCE is very small, despite the quadrupling of the concentration used. This suggests that with the current parameters, concentration may no longer play a role in improving the coverage. Further optimisations of other parameters (e.g. sonication power), along with the concentration, are necessary for improving the film coverage.

Table S1. % Coverage based on cyclic voltammograms. Peak heights were determined as described by Elgrishi et al. [8]

Sample	Coverage (%)
Th-SnO_2	40.7
15-SnO_2	61.7
30-SnO_2	80.5 (Figure 2a), 75.0 (Figure S2)
45-SnO_2	79.0

Table S2: Quantification table for the XPS data shown in Figure 3.

Sample	Sn (at%)	O (at%)	Cl (at%)		O (I) (%)	O (II) (%)
Uncoated	14.13	85.87	0.00		29.23	70.77
Th-SnO_2	22.51	76.72	0.17		43.00	57.00
15-SnO_2	28.19	69.90	1.91		54.81	45.19
30-SnO_2	28.42	69.73	1.85		57.37	42.63
45-SnO_2	30.40	69.16	0.44		61.86	38.14

References

1 T. I. Alanazi, O. S. Game, J. A. Smith, R. C. Kilbride, C. Greenland, R. Jayaprakash, K. Georgiou, N. J. Terrill and D. G. Lidzey, *RSC Adv.*, 2020, **10**, 40341–40350.

2 J. M. C. da Silva Filho and F. C. Marques, *MRS Adv.*, 2018, **3**, 1843–1848.

3 Q. Jiang, L. Zhang, H. Wang, X. Yang, J. Meng, H. Liu, Z. Yin, J. Wu, X. Zhang and J. You, *Nat. Energy*, 2016, **2**, 1–7.

4 E. H. Anaraki, A. Kermanpur, L. Steier, K. Domanski, T. Matsui, W. Tress, M. Saliba, A. Abate, M. Grätzel, A. Hagfeldt and J.-P. Correa-Baena, *Energy Environ. Sci.*, 2016, **9**, 3128–3134.

5 J. A. Smith, O. S. Game, J. E. Bishop, E. L. K. Spooner, R. C. Kilbride, C. Greenland, R. Jayaprakash, T. I. Alanazi, E. J. Cassella, A. Tejada, G. Chistiakova, M. Wong-Stringer, T. J. Routledge, A. J. Parnell, D. B. Hammond and D. G. Lidzey, *ACS Appl. Energy Mater.*, 2020, **3**, 5552–5562.

6 Y. Ko, Y. Kim, C. Lee, T. Kim, S. Kim, Y. J. Yun, H. Gwon, N.-H. Lee and Y. Jun, *ChemSusChem*, 2020, **13**, 4051–4063.

7 H. Uchiyama, H. Ohgi and H. Imai, *Cryst. Growth Des.*, 2006, **6**, 2186–2190.

8 N. Elgrishi, K. J. Rountree, B. D. McCarthy, E. S. Rountree, T. T. Eisenhart and J. L. Dempsey, *J. Chem. Educ.*, 2018, **95**, 197–206.